Citation: Clin Transl Sci (2022) 15, 567–575; doi:10.1111/cts.12798

ARTICLE

MicroRNA-100 Enhances Autophagy and Suppresses Migration and Invasion of Renal Cell Carcinoma Cells via Disruption of NOX4-Dependent mTOR Pathway

Xiumin Liu[1], Lili Zhong[2], Ping Li[3] and Peng Zhao[4,*]

Renal cell carcinoma (RCC) is the most common kidney malignancy and has a poor prognosis owing to its resistance to chemotherapy. Recently, microRNAs (miRNAs or miRs) have been shown to have a role in cancer metastasis and potential as prognostic biomarkers in cancer. In the present study, we aim to explore the potential role of miR-100 in RCC by targeting nicotinamide adenine dinucleotide phosphate oxidase 4 (NOX4) through the mammalian target of rapamycin (mTOR) pathway. Initially, microarray-based gene expression profiling of RCC was used to identify differentially expressed genes. Next, the expression of miR-100 and NOX4 was examined in RCC tissues and cell lines. Then, the interaction between miR-100 and NOX4 was identified using bioinformatics analysis and dual-luciferase reporter assay. Gain-of-function or loss-of-function approaches were adopted to manipulate miR-100 and NOX4 in order to explore the functional roles in RCC. The results revealed the presence of an upregulated NOX4 and a downregulated miR-100 in both RCC tissues and cell lines. NOX4 was verified as a target of miR-100 in cells. In addition, overexpression of miR-100 or NOX4 silencing could increase autophagy while decreasing the expression of mTOR pathway-related genes and migration and invasion. Conjointly, upregulated miR-100 can potentially increase the autophagy and inhibit the invasion and migration of RCC cells by targeting NOX4 and inactivating the mTOR pathway, which contributes to an extensive understanding of RCC and may provide novel therapeutic options for this disease.

Study Highlights

WHAT IS THE CURRENT KNOWLEDGE ON THE TOPIC?
☑ Renal cell carcinoma (RCC) is the most common kidney malignancy and has a poor prognosis owing to its resistance to chemotherapy. Recently, microRNAs (miRNAs) have been shown to have a role in cancer metastasis and potential as prognostic biomarkers in cancer. It has been reported that RCC-associated mammalian target of rapamycin (mTOR) and PIK3CA are genes in the mTOR pathway, and they interact with nicotinamide adenine dinucleotide phosphate oxidase 4 (NOX4). Besides, mTOR pathway activation correlates to RCC.

WHAT QUESTION DID THIS STUDY ADDRESS?
☑ The study focuses on the regulatory mechanism of miR-100 in RCC by mediating the NOX4-independent mTOR pathway.

WHAT DOES THIS STUDY ADD TO OUR KNOWLEDGE?
☑ The miR-100 can inhibit the *NOX4* gene and mTOR pathway, thus enhancing autophagy and impeding invasion and migration of RCC cells.

HOW MIGHT THIS CHANGE CLINICAL PHARMACOLOGY OR TRANSLATIONAL SCIENCE?
☑ miR-100 may be a new target to combat RCC.

Renal cell carcinoma (RCC) is a cancer originating from renal epithelium and accounts for < 90% of kidney cancers.[1] RCC expands over abundant highly heterogenous malignancies in the human kidney with about 202,000 newly diagnosed cases and 102,000 casualties annually.[2] RCC ranks as the 9th most prevalent cancers in men and the 14th most prevailing malignant tumor in women.[3] No apparent symptoms or any laboratory abnormalities are detectable at the very early phase of RCC.[4] Several therapeutic protocols have been developed for RCC in the clinical setting, such as targeted therapy[5] and surgical resection, which presents with an excellent long-term disease-free survival, whereas 20–50% of patients have manifested metastasis or local recurrence after resection solemnly.[6] Smoking, obesity, hypertension, and diabetes mellitus have been identified as vital risk factors for extensive recurrence after treatment in patients with RCC.[5]

The aberrant expression of microRNAs (miRNAs or miRs) can facilitate RCC growth and metastasis and can fundamentally serve as potential biomarkers for RCC.[7] An

[1]Department of Clinical Laboratory, The Second Hospital of Jilin University, Changchun, China; [2]Jilin Provincial Key Laboratory on Molecular and Chemical Genetic, The Second Hospital of Jilin University, Changchun, China; [3]Department of Developmental Pediatrics, The Second Hospital of Jilin University, Changchun, China; [4]Department of Anesthesiology, The Second Hospital of Jilin University, Changchun, China. *Correspondence: Peng Zhao (zhaopeng_zp@126.com)
Received: December 23, 2019; accepted: March 4, 2020. doi:10.1111/cts.12798

existing study flagged the functionality of miR-100 as a vital prognostic marker for RCC due to the strong association of its overexpression with advanced tumor progression and unfortunate clinical outcomes of patients with RCC.[8] Moreover, miR-100 can comprehensively inhibit cell growth and proliferation by repressing its target gene HOXA1 in nasopharyngeal carcinoma.[9] The bioinformatics prediction website TargetScan (www.targetscan.org) revealed nicotinamide adenine dinucleotide phosphate oxidase 4 (NOX4) as a direct target gene of miR-100. NOX4 is the only NOX isoform that is apparently expressed in human primary chondrocytes among the seven nicotinamide adenine dinucleotide phosphate oxidases expressed in humans.[10] NOX4 fundamentally functions as a sensor for oxygen, and a regulator for controlling vasoconstriction, cell proliferation, migration, and apoptosis,[11] and loss of function of NOX4 is a precursor of tumor aggressiveness.[12] NOX4 silencing can extensively impair cell invasion, colony formation, and growth in a murine xenograft model RCC.[13] Additionally, NOX4-induced reactive oxygen species production is paralleled by activation of the mammalian target of rapamycin (mTOR) pathway, thus exacerbating colorectal cancer malignancy in a diabetic milieu.[14] Accumulating evidence has demonstrated the vitality of the activated mTOR pathway on the progression of RCC.[15] Therefore, we hypothesized the potential of miR-100 to downregulate NOX4 and consequently regulate the mTOR pathway, thereby participating in the progression of RCC. Hence, this study was planned to confirm this hypothesis.

METHODS

Ethics statement

The study was conducted with approval of the Institutional Review Board of the Second Hospital of Jilin University and strict accordance with the Declaration of Helsinki. All participants provided written informed consents before sample collection.

Microarray-based gene expression profiling

The GSE77199 dataset was downloaded from the Gene Expression Omnibus database in National Center for Biotechnology Information (NCBI; http://www.ncbi.nlm.nih.gov/geo/) and the chosen annotation platform was GPL14550-Agilent-028004 SurePrint G3 Human GE 8x60K Microarray (Probe Name Version). The dataset consisted of a combination of four normal kidney endothelial samples and four RCC endothelial samples. The Affy package of R language was adopted for background correction, log2 conversion and standardization of the expression matrix data,[16] and the Limma package of R language was applied in order to screen the differentially expressed genes related to RCC with P value < 0.05 and |LogFoldChange| > 1 as the preliminary threshold.[17] Gene-disease database DisGeNET (http://www.disgenet.org/web/DisGeNET/menu/search?4) was utilized to study the genes, and predict and verify the molecular mechanism of human diseases,[18] which was adopted in the current study in an attempt to retrieve RCC-associated genes with "renal cell carcinoma" as the key word. The STRING (https://string-db.org/) database contains relevant information on the protein interaction relationship and protein function information[19] and is often used for the analysis to the relationship between RCC-associated differentially expressed genes and disease genes and Kyoto Encyclopedia of Genes and Genomes pathway enrichment analysis. The protein-protein interaction (PPI) network was constructed and visualized using the Cytoscape 3.6.0 software,[20] after which the key differential genes related to RCC were confirmed. Next, the miRNAs, which potentially regulate the differentially expressed genes, were predicted using the microRNA (http://34.236.212.39/microrna/getGeneForm.do), mirDIP (http://ophid.utoronto.ca/mirDIP/), and miRSearch 3.0 (http://www.exiqon.com/microrna-target-prediction) and then compared by Venn online analysis tool Calculate and draw custom Venn diagrams (http://bioinformatics.psb.ugent.be/webtools/Venn/).

Study subjects

From a period of September 2008 to October 2016, fresh tumor tissues and adjacent normal tissues (5 cm away from the tumor tissues) were isolated and collected from 113 patients with RCC who underwent radical nephrectomy at the Second Hospital of Jilin University. Among the 113 patients, there were 78 men and 35 women aged 24–73 years with an average age of 61 years. They were categorized into stage I–II (n = 67) and stage III–IV (n = 44) in strict accordance with the classification standard of the 2002 American Joint Committee on Cancer tumor-nodes-metastasis (AJCC TNM).[21] The fresh pathological tissue samples of patients were frozen using liquid nitrogen and stored at −80°C for subsequent experiment. No patient was instilled radiotherapy, chemotherapy, or other treatments prior to the operation.

Hematoxylin-eosin staining

RCC and adjacent normal tissue samples were fixed using 4% paraformaldehyde (p1110-100, Tideradar Beijing Technology, Beijing, China) and then dissected into 4-μm sections. The sections were then subjected to hematoxylin-eosin (H&E) staining and observed under an optical microscope (XSP-8CA; Shanghai Optical Instrument Factory, Shanghai, China).

Reverse transcription quantitative polymerase chain reaction

Total RNA was extracted from the tissues and cells using the TRIzol reagent (16096020; Thermo Fisher Scientific, New York, NY). The purity and concentration of the extracted RNA were determined using an ultraviolet spectrophotometer (DU640; Backman, Fullerton, CA). The mRNA was then reversely transcribed into complementary DNA using the PrimeScript RT reagent Kit (TaKaRa Bio, Shiga, Japan). The miRNA First Strand cDNA Synthesis (Tailing Reaction) kit (B532451-0020; Shanghai Sangon Biotech, Shanghai, China). The SYBR Green fluorescent dye method was adopted for reverse transcription quantitative polymerase chain reaction (RT-qPCR). The primer sequences for miR-100, NOX4, mTOR, LC3, matrix metalloproteinase (MMP)-2, and MMP-9 are shown in **Table 1**, with U6[22] and β-actin serving as internal references of the miRNA and mRNA separately. The relative expression of genes was

Table 1 Primer sequences for RT-qPCR

Genes	Primer sequence (5′-3′)
miR-100	F: GCGGCAACCCGTAGATCCCAA
	R: GTGCAGGGTCCGAGGT
NOX4	F: GCTGACGTTGCATGTTTCAG
	R: CGGGAGGGTGGGTATCTAA
mTOR	F: CGGGGTACCAGATGTGCCCATCACGTTTT
	R: CCGGAATTCTGGTGTCTAGACATGGCTACACTT
S6K1	F: AGACGGGAAGCGATAAGGAAAGCA
	R: TCAGCCTTAGTGTGTGCAGTGTCT
LC3	F: CATCACAGTTGGCACAAACG
	R: AGTGAGGACTTTGGGTGTGG
MMP-2	F: GCTACCACCTACAACTTTGAGAA
	R: TGTCATAGGATGTGCCCTGGAA
MMP-9	F: TGGGCTGCTGCTTTGCT
	R: GCCTGTCGGTGAGATTGGTT
U6	F: CTCGCTTCGGCAGCACA
	R: AACGCTTCACGAATTTGCGT
β-actin	F: AGGGGCCGGACTCGTCATACT
	F: GGCGGCACCACCATGTACCCT

β-actin, beta-actin; F, forward; LC3, light chain 3; miR-100, microRNA-100; MMP, matrix metalloproteinase; mTOR, mammalian target of rapamycin; NOX4, nicotinamide adenine dinucleotide phosphate oxidase 4; R, reverse; RT-qPCR, reverse transcription quantitative polymerase chain reaction; S6K1, ribosomal protein S6 kinase beta-1.

calculated based on the $2^{-\Delta\Delta Ct}$ method and the formula was as follows: $\Delta\Delta Ct = \Delta Ct$ (RCC group) – $\triangle Ct$ (normal group), ΔCt = CT (target genes) – CT (internal references). The aforementioned protocol was also used in the following cell experiments.

Western blot analysis

A total of 50 mg frozen RCC and adjacent normal tissues were supplemented with 500 μL radioimmunoprecipitation assay lysis buffer (Pierce, Rockford, IL), and left to stand over ice for 60 minutes. The solution was cooled down, transferred to a 1.5 mL Eppendorf tube, and centrifuged at 6,037.2 g and 4°C for 30 minutes, with collection of the supernatant. The protein concentration was then detected using a bicinchoninic acid kit (BCA1-1KT; Sigma-Aldrich Chemical, St. Louis, MO). The protein was then separated by performing sodium dodecyl sulfate-polyacrylamide gel electrophoresis and transferred onto membranes. A membrane blockade was conducted using 5% skimmed milk and subsequently probed with the following rabbit anti-human primary antibodies: NOX4 (ab133303, 1: 1000; Abcam, Cambridge, UK), mTOR (ab2732, 1: 1000, Abcam), LC3 (ab48394, 1: 1000; Abcam), MMP-2 (ab37150, 1: 1000; Abcam), MMP-9 (ab73734, 1: 1000; Abcam), S6K1 (ab32529, 1: 5000; Abcam), and glyceraldehyde 3-phosphate dehydrogenase ABP57259, 1: 5000; Abbkine Scientific, Wuhan, China) overnight at 4°C. Next, the membrane was re-probed with the horseradish peroxidase-labeled secondary goat anti-rabbit antibody (A0208; Beyotime Biotechnology, Shanghai, China) at 37°C for 45 minutes. The immunocomplexes on the membrane were visualized using the enhanced chemiluminescence reagent (ECL808-25; Biomiga, San Diego, CA) for 1 minute with quantification of the band intensities using the Gel-Pro Analyzer 4.0 software (Media Cybernetics, Rockville, MD). The relative protein expression was denoted as the ratio of the gray value of the target band to glyceraldehyde 3-phosphate dehydrogenase.

Dual-luciferase reporter assay

NOX4 was introduced into pMIR-reporter with the endonuclease sites Spe I and Hind III, and the complementary sequence mutation sites of seed sequence was designed on pNOX4-wide type (wt) to establish pNOX4-mutant (mut). The dual-luciferase reporter plasmids NOX4 wt and NOX4 mut with the correct identification sequences were respectively transfected with miR-100 mimic or negative control (NC) mimic into the HEK-293T cells (CRL-1415; Shanghai Xin Yu Biotech, Shanghai, China). The dual-luciferase report assay kit (RG005; Beyotime Biotechnology) was used so as to dissolve the Renilla luciferase assay buffer and firefly luciferase detection agent separately. The Renilla luciferase served as the internal reference.

Plasmid construction

The NOX4-short hairpin RNA (shRNA) sequence (sense: 5′-CACCGCACTGTGTCGAAGAATTTACCGAAGTAA ATTCTTCGACACAGTGC-3′; anti-sense: 5′-AAAAGCACT GTGTCGAAGAATTTACTTCGGTAAATTCTTCGACACAG TGC-3′) was designed by the online design website of the Thermo Fisher Corporation according to the mRNA complete sequences of NOX4 (NM_001291929) as reported in GenBank and the short hairpin RNA (shRNA) design principles. All shRNA oligonucleotides fragments were synthesized by Shanghai Sangon Biological Engineering Technology Service (Shanghai, China). Later, the aforementioned fragments were introduced into the carrier pSIREN (HAB 2-9; Beijing Hua'ao Zhengsheng Technology, Beijing, China), which had been linearized by BamHI and EcoRI (ER0052, ER0271; Cobioer Biosciences, Nanjing, China). After annealing, the carrier was transfected into Escherichia coli DH5, and the resistant colony of penbritin was chosen for amplification and cultured after construction of the recombinant vectors pSI-REN/S and pSIREN/CN. A small number of plasmids were prepared promptly with identification of its nucleic acid sequence, and the clone with the correct identification sequence was chosen for subsequent amplification and culture.

Cell culture and transfection

Human RCC cell lines ACHN, A498, CAKI-1, and 786-0, were acquired from Cell Resource Center of Shanghai Institutes for Biological Sciences of Chinese Academy of Sciences. All cells were cultured using Dulbecco's modified Eagle's medium (DMEM; Hyclone, Logan, UT) containing 10% fetal bovine serum in a 5% CO_2 incubator at 37°C. The DMEM culture medium was supplemented with 100 U penicillin and 100 mg streptomycin (Gibco, Grand Island, NY).

The ACHN and A498 cell lines were extracted and allocated into six groups: the blank group (without any transfection), the miR-100 mimic group (transfected with miR-100 mimic sequences (10 μmol/L, 5 μL)), the miR-100 inhibitor group

(transfected with miR-100 inhibitor sequences (10 μmol/L, 10 μL), GenePharma (Shanghai, China)), the NC group (transfected with miR-100 NC sequences (10 μmol/L, 5 μL), GenePharma (Shanghai, China)), the shRNA-NOX4 group (transfected with shRNA-NOX4 plasmids), and the miR-100 inhibitor + shRNA-NOX4 group (transfected with miR-100 inhibitor sequences and shRNA-NOX4 plasmids). The target sequences were purchased from Shanghai GenePharma. Cell transfection was performed using Lipofectamine 2000 (11668019; Thermo Fisher Scientific) in compliance with the provided instructions. The transfection sequences are shown in **Table 2**.

Transwell assay

The Matrigel gel (356234; Becton, Dickinson and Company, Franklin Lakes, NJ) and serum-free medium Roswell Park Memorial Institute (RPMI) 1640 (Gibco) were diluted at a ratio of 1:1, which were then added to the upper Transwell chamber at a density of 50 μL per well at 37°C for 3 hours. The transfected ACHN cells in each group were isolated using 0.25% trypsin, suspended, centrifuged at 25,764 *g* for 10 minutes, and later amassed. The cells were diluted to a concentration of 3×10^4/mL using serum-free RPMI 1640 (Gibco). In each group, 3 duplicated wells were set, and 200 μL cell suspension was added to the upper Transwell chamber, and serum-free medium was supplemented into the lower Transwell chamber, followed by 48-hour culture in conventional conditions. The filter membrane was then removed and the cells failing to infiltrate the micropore were wiped off with cotton swabs, after which the remaining cells were stained with 0.1% crystal violet for 10 minutes. Next, the number of cells successfully passing through the membrane was calculated from five randomly selected fields under a microscope to assess the invasive ability.

Scratch test

The transfected cells in each group were inoculated in a 6-well plate at a density of 2×10^5 cells per well. Upon attaining 80–90% confluence of adherent cells, a 200 μL pipette tip was used to scratch the well slightly and vertically along the axis of the well. The floating cells were rinsed twice with phosphate-buffered saline (PBS), and the remaining cells were supplemented with serum-free RPMI 1640 medium and incubated for 0.5–1 hour as part of the recovery process. The cells were then photographed at 0 and 24 hours after transfection and the Image-Pro Plus Analysis software (Media Cybernetics, Rockville, MD) was used to measure the distance of cell migration (cell migration distance = initial scratch width – scratch width).

Green fluorescent protein-light chain 3 method

Cell culture dishes in each group were covered using cover glasses. Upon attaining 70% confluence, the culture medium was removed. Then, 2 μg green fluorescent protein-light chain 3 (GFP-LC3) plasmids (24920; Addgene Plasmid Bank, Watertown, MA) and 5 μL Lipofectamine 2000 (Invitrogen, Carlsbad, CA) were separately mixed with 100 μL serum-free DMEM, and allowed to stand for 45 minutes, followed by incubation in a 5% CO_2 incubator at 37°C for 8 hours, and another 24 hours of incubation with replacement of the original complete medium. Later, the cultured cells were fixed using 4% poly methanol for 30 minutes and rinsed with PBS 3 times (5 minutes each time). After being mounted with glycerol, the cells were observed under a fluorescence microscope. At last, the formation of the autophagic vacuole in cells and the number of the GFP-LC3 fluorescent spots of cells in each group was observed and documented under multiple randomly selected fields.

Monodansylcadaverine fluorescence staining method

The sterilized cover glasses (24 × 24 mm) were placed onto the culture dishes to inoculate the cell lines in each group, which extended on the slide and incubated for 24 hours. Upon reaching 70% confluence, the cells were supplemented with 0.05 mmol/L monodansylcadaverine (Sigma-Aldrich Chemical Company), incubated with 5% CO_2 under conditions devoid of light for 20 minutes at 37°C, and rinsed with PBS 3 times (5 minutes each time). Then, the cells were fixed using 95% alcohol for 15 minutes, rinsed with PBS 3 times (5 minutes each time), incubated with 5 μmol/LPI for 10 minutes at room temperature, and then rinsed again with PBS 3 times (5 minutes each time). After exposure in a well-ventilated place, the fluorescent spots of the cells were photographed and counted under a fluorescence microscope.

Statistical analysis

All experimental data were analyzed using the SPSS 21.0 statistical software (IBM, Armonk, NY). Each experiment was repeated for three times independently. With the mean values obtained, the measurement data were expressed as mean ± SD. Comparison for data between the two groups was performed based on the *t*-test, and comparison among multiple groups was conducted by one-way analysis of variance. The numerical data were presented as percentage, and compared by the χ^2 test. A value of $P < 0.05$ was considered to be indicative of statistical significance.

Table 2 Sequences for miR-100 mimic, miR-100 inhibitor, and miR-100 NC

Item	Sequence (5′-3′)
miR-100 mimic	GGUCUUCGGTGTTTGGGCUTCTUGGCTTGUUCUCCUTUUTCUGGCGTGTTCGUUCUTUGUTUTCCUTUCUCUGUCUUTCC
miR-100 inhibitor	CCTUUCUGUCUCUTUCCTUTUGUTUCUUGCTTGTGCGGUCTUUTUCCUCUUGTTCGGUTCTUCGGGTTTGTGGCUUCUGG
miR-100 NC	UUCUCCGAACGUGUCACGUTT

miR-100, microRNA-100; NC, negative control.

RESULTS

Bioinformatic analysis to predict the differentially expressed genes and their molecular interactions in RCC

We first performed a differential gene expression analysis on an RCC-related expression dataset GSE77199 downloaded from the Gene Expression Omnibus (http://www.ncbi.nlm.nih.gov/geo/) with P value < 0.05 and |Log FoldChange| > 1 as the threshold. A heat map illustrating the first 10 most differentially expressed genes is shown in **Figure a1**. In addition, the first 20 genes related to RCC were retrieved from the DisGeNET database, which were subjected to a regimen of gene interaction analysis together with adopting the exceeding 10 genes for constructing a PPI network. **Figure a1** shows that NOX4 expressed to a higher extent in RCC tissues than the healthy renal tissues, indicating a change in NOX4 expression might influence RCC. In addition, the PPI network showed that the differentially expressed NOX4 gene candidly interacted with multiple RCC genes (**Figure b1**). In **Figure c1**, RCC-associated genes *mTOR* and *PIK3CA* were the interactive genes in the mTOR pathway responsible for the interaction with NOX4. Activation of the mTOR pathway is related to RCC[23,24] and NOX4 activates the mTOR pathway.[25] The aforementioned results suggested that the upregulated NOX4 activated the mTOR pathway in RCC. A total of 49, 34, and 62 miRNAs regulating NOX4 were

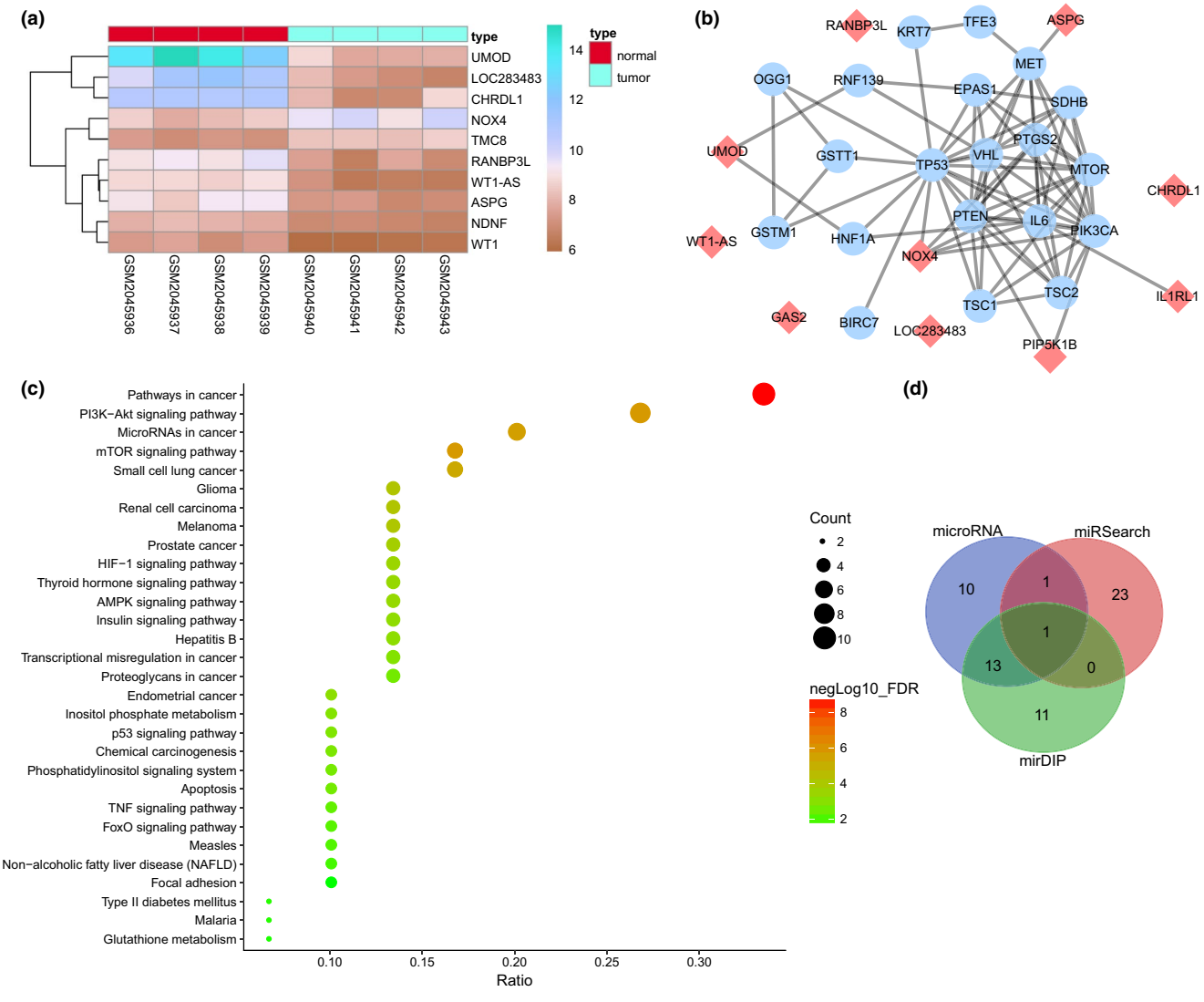

Figure 1 Bioinformatics predicates that microRNA (miR-100) regulated renal cell carcinoma (RCC) by targeting nicotinamide adenine dinucleotide phosphate oxidase 4 (NOX4) through mammalian target of rapamycin (mTOR) pathway. (**a**) A heat map depicting the first 10 differentially expressed genes in the GSE77199 dataset, in which abscissa represented sample number and ordinate represented differentially expressed genes; the histogram at the upper right was the color gradation, and each rectangle in this histogram corresponded to a sample expression value; red color represented normal samples, and blue represented RCC samples; blue represented high expression, and pink represented low expression; (**b**) the protein-protein interaction) network of RCC-related differentially expressed genes and RCC genes, in which red diamond represented differentially expressed genes and blue circle represented RCC gene; (**c**) the enrichment of Kyoto Encyclopedia of Genes and Genomes pathway regarding the RCC-related differentially expressed genes; (**d**) possible miRNAs regulating NOX4 predicted by microRNA, mirDIP, and miRSearch.

predicted by the microRNA (http://34.236.212.39/microrna/getGeneForm.do), mirDIP (http://ophid.utoronto.ca/mirDIP/) and miRSearch (http://www.exiqon.com/microrna-target-prediction). Twenty-five miRNAs from each prediction were selected and paralleled, after which a Venn diagram (http://bioinformatics.psb.ugent.be/webtools/Venn/) was plotted (**Figure d1**), which showed only one miRNA intersected hsa-miR-100-5p, thereby suggesting that hsa-miR-100-5p was capable of targeting NOX4 independently. Moreover, existing studies have indicated that miR-100 inhibited the mTOR pathway.[26,27] Therefore, we elucidated that miR-100 affected RCC by targeting NOX4 via the mTOR pathway.

H&E staining analysis of RCC tissues

H&E staining results showed that the nucleus was profoundly expressive with significant abnormal and disordered forms, attenuated cytoplasm, and unapparent interstitial vessels in the RCC tissues compared with the adjacent normal tissues (**Figure 2**).

RCC tissues showed increased expression of NOX4, mTOR, S6K1, MMP-2, and MMP-9 but decreased expression of miR-100 and LC3

The results detected by means of RT-qPCR indicated that, compared with the adjacent normal tissues, the mRNA expression of NOX4, mTOR pathway-related genes (mTOR and S6K1), cell invasion-related, and migration-related genes (MMP-2 and MMP-9) was significantly elevated, whereas miR-100 expression and autophagy-related gene (LC3) mRNA expression were significantly lessened in RCC tissues ($P < 0.05$; **Figure 3**).

RCC tissues had significantly elevated protein expression of NOX4, mTOR, p-mTOR, S6K1 and p-S6K1, MMP-2, and MMP-9, whereas lowered LC3-II/LC3-I expression

The results from Western blot analysis showed that the protein expression of NOX4, mTOR pathway-related (mTOR, p-mTOR, S6K1, and p-S6K1), cell invasion-related and migration-related genes (MMP-2 and MMP-9) was notably higher, whereas that of autophagy-related genes (ratio between LC3-II and LC3-I) was lower in RCC tissues than the adjacent normal tissues ($P < 0.05$; **Figure 4**).

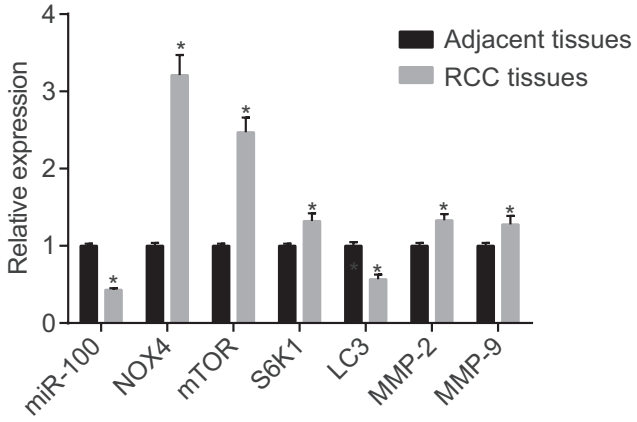

Figure 3 Renal cell carcinoma (RCC) tissues revealed higher mRNA expression of nicotinamide adenine dinucleotide phosphate oxidase 4 (NOX4), mammalian target of rapamycin (mTOR), S6K1, matrix metalloproteinase (MMP)-2, and MMP-9, yet lower microRNA (miR)-100 and light chain 3 (LC3) expression. * $P < 0.05$ compared to the adjacent normal tissues.

miR-100 negatively targeted NOX4

NOX4 was verified as a target gene of miR-100 according to the online prediction website Target Scan (**Figure a5**). Results of the dual-luciferase reporter assay (**Figure b5**) showed that compared with the NC group, the luciferase signal of NOX4-wt was decreased ($P < 0.05$), whereas that of the luciferase signal of NOX4-mut exhibited no evident differences ($P > 0.05$) in cells transfected with the miR-100 mimic. These findings indicated that miR-100 could precisely bind with the *NOX4* gene and subsequently inhibit its expression ($P < 0.05$).

NOX4 expressed the highest in ACHN and 786-0 cell lines

The expression of NOX4 was quantified in five RCC cell lines (ACHN, A498, CAKI-2, 786-0, and CAKI-1). The results showed that the expression of NOX4 in the A498, CAKI-2, and CAKI-1 cell lines was significantly lower compared with the ACHN and 786-0 cell lines ($P < 0.05$; **Figure S1**). Therefore, the ACHN and 786-0 cell lines were chosen for subsequent experimentation.

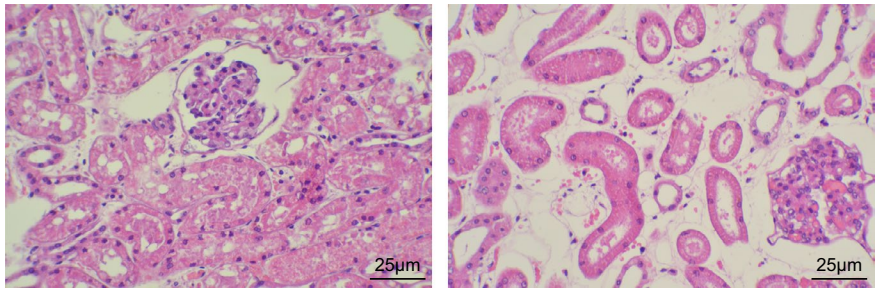

Adjacent tissues RCC tissues

Figure 2 Pathological features of renal cell carcinoma (RCC) tissues and adjacent normal tissues examined by hematoxylin-eosin staining under an optical microscope (400×). The images represented the hematoxylin-eosin staining analysis of RCC tissues and adjacent normal tissues.

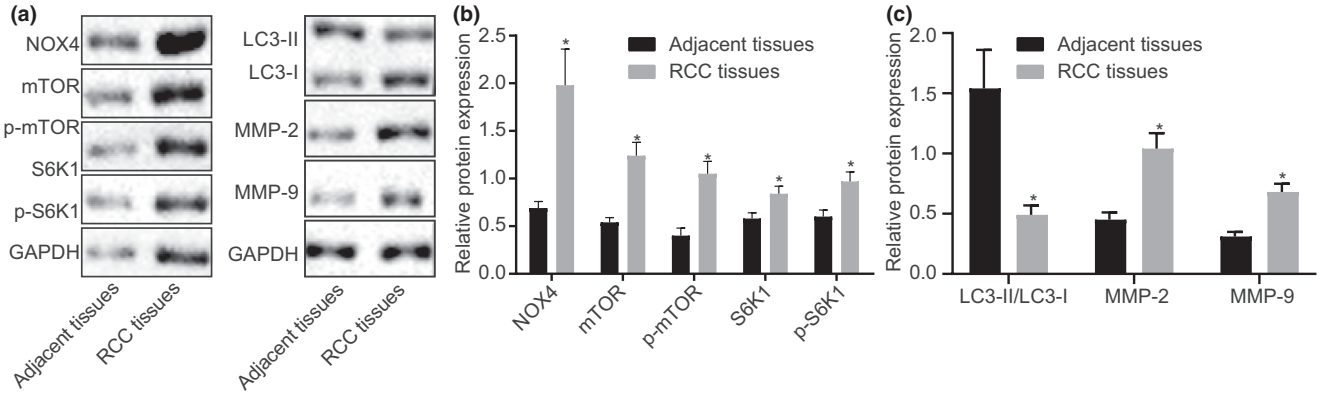

Figure 4 Increased protein expression of nicotinamide adenine dinucleotide phosphate oxidase 4 (NOX4), mammalian target of rapamycin (mTOR), S6K1, matrix metalloproteinase (MMP)-2, and MMP-9, as well as extent of mTOR and S6K1 phosphorylation, yet decreased light chain 3 (LC3)-II/LC3-I in renal cell carcinoma (RCC) tissues. (**a**) Grey value analysis of NOX4, mTOR, S6K1, MMP-2, MMP-9, extent of mTOR and S6K1 phosphorylation, and LC3-II/LC3-I detected by Western blot analysis; (**b, c**) relative protein expression of NOX4, mTOR, S6K1, MMP-2, MMP-9, and LC3-II/LC3-I, as well as the extent of mTOR and S6K1 phosphorylation detected by Western blot analysis; $^{*}P < 0.05$ compared to the adjacent normal tissues. GADPH, glyceraldehyde 3-phosphate dehydrogenase.

miR-100 overexpression downregulated NOX4 and inhibited the mTOR pathway

After transfection, RT-qPCR and Western blot analysis were conducted for detection of the relative expression, the results of which indicated that the ACHN and 786-0 cell lines had the same tendency. As shown by **Figures S2** and **S3,** no statistical difference was observed in the miR-100 expression, mRNA, and protein expression of NOX4, mTOR, S6K1, LC3, LC3-II/LC3-I, MMP-2, and MMP-9, as well as the extent of mTOR and S6K1 phosphorylation between the blank group and the NC group ($P > 0.05$). In comparison to the blank and NC groups, the miR-100 mimic group presented with lower mRNA and protein expression of NOX4, mTOR, S6K1, MMP-2, and MMP-9, as well as lower extent of mTOR and S6K1 phosphorylation but higher expression of miR-100, LC3, and LC3-II/LC3-I ($P < 0.05$). The expression of miR-100, LC3, and LC3-II/LC3-I was lowered, whereas the expression of NOX4, mTOR, SK61, MMP-2, and MMP-9, and the extent of mTOR and S6K1 phosphorylation were upregulated in the miR-100 inhibitor group in comparison to the blank and NC groups (all $P < 0.05$). No significant different miR-100 expression ($P > 0.05$) was evident in the shRNA-NOX4 group, with lower mRNA and protein expression of NOX4, mTOR, S6K1, MMP-2, and MMP-9, as well as lower extent of mTOR and S6K1 phosphorylation but higher expression of LC3 and LC3-II/LC3-I in relation to the blank and NC groups ($P < 0.05$). The miR-100 inhibitor + shRNA-NOX4 group exhibited lower expression of miR-100 ($P < 0.05$) and insignificantly different expression of NOX4, mTOR, S6K1, LC3, MMP-2, MMP-9, and extent of mTOR and S6K1 phosphorylation in comparison with the blank and NC groups ($P > 0.05$).

miR-100 inhibited the invasion and migration of RCC cells by downregulating NOX4

Transwell assay (**Figure S4**) and scratch test (**Figure S5**) results showed that the invasive and migration abilities of ACHN and 786-0 cells were not substantially different between the

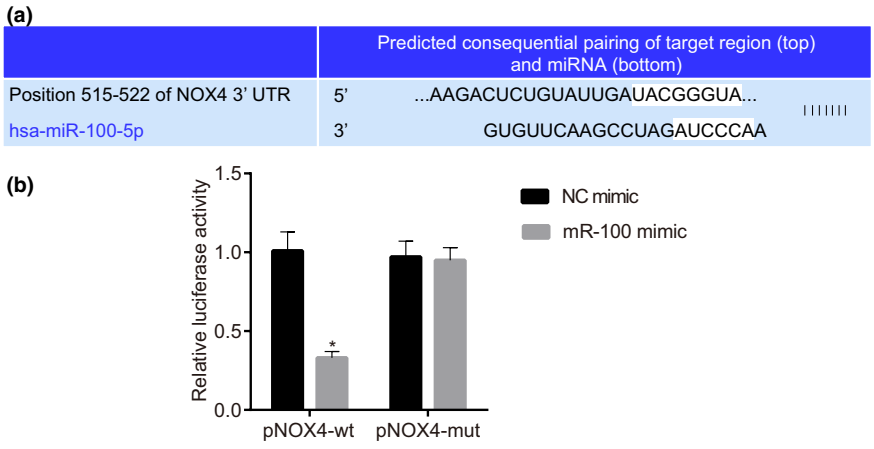

Figure 5 Nicotinamide adenine dinucleotide phosphate oxidase 4 (NOX4) was a target gene of microRNA (miR)-100. (**a**) The predicted binding sites between miR-100 and NOX4 3′ untranslated region (UTR); (**b**) the binding of miR-100 to NOX4 examined by dual-luciferase reporter assay; $^{*}P < 0.05$ compared to the negative control (NC) mimic group. mut, mutant; wt, wide type.

blank group and the NC group ($P > 0.05$). In comparison with the NC and blank groups, the miR-100 inhibitor + shRNA-NOX4 group also showed no obvious difference regarding the invasive and migration abilities of the ACHN and 786-0 cells ($P > 0.05$). However, the invasive and migration abilities of ACHN and 786-0 cells were significantly elevated in the miR-100 inhibitor group and markedly lowered in the shRNA-NOX4 and miR-100 mimic groups compared with the NC and blank groups (all $P < 0.05$). The collected data demonstrated that impelled miR-100 could impair the invasion and migration of RCC cells by downregulating NOX4.

miR-100 promoted the autophagy of RCC cells by repressing NOX4

We adopted the GFP-LC3 and monodansylcadaverine procedures to detect the autophagy of ACHN and 786-0 cells. Under a fluorescence microscope, a fluorescent spot represented the autophagosome, with the increased fluorescent spot denoting enhanced autophagic ability. As shown in **Figure S6,** no significant changes were observed in the autophagic ability of cells between the NC group and the blank group ($P > 0.05$). No evident alterations in the autophagic ability of cells were detected among the miR-100 inhibitor + shRNA-NOX4, NC, and blank groups ($P > 0.05$). In comparison to the NC and blank groups, the autophagic ability of cells was significantly increased in the miR-100 mimic and shRNA-NOX4 groups, whereas the ability was notably decreased in the miR-100 inhibitor group ($P < 0.05$). The aforementioned data exhibited that miR-100 accelerated autophagy of RCC cells via suppression of NOX4.

DISCUSSION

The application of miRNAs as potential biomarkers and therapy targets has undergone extensive investigation in several kinds of cancers.[28] In this study, we elucidated the capability of miR-100 to inhibit the growth of RCC cells by suppression of the mTOR pathway via targeting NOX4.

Our study showed low expression of miR-100 and high expression of NOX4 and mTOR in both RCC tissues and cell lines. A reduced miR-100 expression is characteristic of several cancers. Specifically, miR-100 was evidently downregulated in human hepatocellular carcinoma tissues.[29] Moreover, in consistency with our study, Wang *et al*. also demonstrated an overexpressed miR-100 in RCC.[8] Several miRNAs can modulate gene expression post-transcriptionally via association with the 3′UTR of specific target mRNAs.[30] In the present study, NOX4 was ascertained as a target gene of miR-100, which could essentially be negatively regulated by miR-100. An existing study demonstrated that NOX4 upregulation is a vital contributor for diabetic nephropathy and can also contribute to tumor cells' progression and metastasis.[31] In accordance with our findings, NOX4 was confirmed as a potential miR-100 target at 3′UTR.[32]

miR-100 has been identified to function as an inhibitor of proliferation, motility, tumorigenicity, and invasiveness of diverse tumor cells through direct targeting of distinct genes.[33] The findings from the present study revealed the inhibitory properties of miR-100 overexpression in suppressing the invasion and migration ability of RCC cells along with the catalytic role in stimulating autophagy by blockage of the mTOR pathway via suppression of NOX4. Similarly, an existing study substantiated the ability of miR-100 overexpression to suppress cell proliferation, invasion, and migration in osteosarcoma by specifically targeting insulin-like growth factor 1 receptor.[34] Additionally, a study documented the overexpression of miR-100 to fundamentally suppress the migration and invasion of breast cancer cells by explicitly targeting FZD-8.[35] Autophagy has been involved in physiological processes as cell development and differentiation in various human diseases, and its effect on tumorigenesis might be inconclusive.[36] Moreover, miR-100 stimulates endothelial autophagy *in vitro* and *in vivo* and consequently suppresses chronic vascular inflammation.[37] NOX4 also serves as a functional regulator in autophagy due to its intracellular localization and its ability to produce hydrogen peroxide intrinsically.[38] NOX4 inhibitors can comprehensively impede activation of the mTOR pathway.[39] The involvement of the mTOR pathway is evident in the pathogenesis of multiple kinds of cancers, including RCC.[40] Specifically, mTOR inhibitors have been extensively adopted as first-line and second-line treatments for RCC.[41] Additionally, the suppressive effect of overexpressed miR-100 on mTOR pathway has been previously documented.[42] Besides, miR-100 has been demonstrated to function as a growth-inhibiting miRNA in several cancers, such as human bladder cancer and osteosarcoma under partial suppression of the mTOR pathway.[26,43,44] On the basis of the aforementioned literature, we can speculate the ability of miR-100 to retard RCC progression via NOX4-dependent mTOR pathway inactivation.

In conclusion, the present study provides evidence supporting the potential of miR-100 to trigger autophagy and curtail the invasion and migration of RCC cells by inhibiting the mTOR pathway through downregulation of NOX4 (**Figure S7**). These findings are expected to provide new treatment targets for the development of efficacious RCC treatment protocols. However, the molecular mechanism of miR-100 in RCC still requires further elucidation in a more comprehensive manner with *in vivo* experimentation in the future.

Supporting Information. Supplementary information accompanies this paper on the *Clinical and Translational Science* website (www.cts-journal.com).

Acknowledgment. The authors would like to express their sincere appreciation to the reviewers for their helpful comments on this article.

Funding. No funding was received for this work.

Conflict of Interest. The authors declared no competing interests for this work.

Author Contributions. P.L. and P.Z. wrote the manuscript. X.L. and P.L. designed the research. L.Z. and P.Z. performed the research. L.Z. analyzed the data. X.L. contributed new reagents/analytical tools.

1. Hsieh, J.J. *et al.* Renal cell carcinoma. *Nat. Rev. Dis. Primers* **3**, 17009 (2017).
2. Yang, T. *et al.* lncRNA PVT1 and its splicing variant function as competing endogenous RNA to regulate clear cell renal cell carcinoma progression. *Oncotarget* **8**, 85353–85367 (2017).

3. Martin, S.S. *et al.* Impact of noise-optimized virtual monoenergetic dual-energy computed tomography on image quality in patients with renal cell carcinoma. *Eur. J. Radiol.* **97**, 1–7 (2017).
4. Wu, H.B. *et al.* Autophagy-induced KDR/VEGFR-2 activation promotes the formation of vasculogenic mimicry by glioma stem cells. *Autophagy* **13**, 1528–1542 (2017).
5. van der Mijn, J.C. *et al.* Validation of risk factors for recurrence of renal cell carcinoma: results from a large single-institution series. *PLoS One* **14**, e0226285 (2019).
6. Chen, X.Y. *et al.* Risk factors for bone metastasis from renal cell cancer. *J. Bone Oncol.* **9**, 29–33 (2017).
7. Lokeshwar, S.D. *et al.* Molecular characterization of renal cell carcinoma: a potential three-microRNA prognostic signature. *Cancer Epidemiol. Biomarkers Prev.* **27**, 464–472 (2018).
8. Wang, G., Chen, L., Meng, J., Chen, M., Zhuang, L. & Zhang, L. Overexpression of microRNA-100 predicts an unfavorable prognosis in renal cell carcinoma. *Int. Urol. Nephrol.* **45**, 373–379 (2013).
9. He, W. *et al.* miR-100 inhibits cell growth and proliferation by targeting HOXA1 in nasopharyngeal carcinoma. *Onco. Targets Ther.* **13**, 593–602 (2020).
10. Morel, F., Rousset, F., Vu Chuong Nguyen, M.,Trocme, C., Grange, L. & Lardy, B. [NADPH oxidase Nox4, a putative therapeutic target in osteoarthritis]. *Bull. Acad. Natl. Med.* **199**, 673–686; discussion 686–677 (2015).
11. Chen, F., Haigh, S., Barman, S. & Fulton, D.J. From form to function: the role of Nox4 in the cardiovascular system. *Front. Physiol.* **3**, 412 (2012).
12. Crosas-Molist, E. *et al.* The NADPH oxidase NOX4 represses epithelial to amoeboid transition and efficient tumour dissemination. *Oncogene* **36**, 3002–3014 (2017).
13. Gregg, J.L. *et al.* NADPH oxidase NOX4 supports renal tumorigenesis by promoting the expression and nuclear accumulation of HIF2alpha. *Cancer Res.* **74**, 3501–3511 (2014).
14. Mroueh, F.M. *et al.* Unmasking the interplay between mTOR and Nox4: novel insights into the mechanism connecting diabetes and cancer. *FASEB J.* **33**, 14051–14066 (2019).
15. Yang, Z., Xie, H., He, D. & Li, L. Infiltrating macrophages increase RCC epithelial mesenchymal transition (EMT) and stem cell-like populations via AKT and mTOR signaling. *Oncotarget* **7**, 44478–44491 (2016).
16. Gautier, L., Cope, L., Bolstad, B.M. & Irizarry, R.A. Affy–analysis of Affymetrix GeneChip data at the probe level. *Bioinformatics* **20**, 307–315 (2004).
17. Smyth, G.K. Linear models and empirical Bayes methods for assessing differential expression in microarray experiments. *Stat. Appl. Genet. Mol. Biol.* **3**, Article3 (2004).
18. Pinero, J. *et al.* DisGeNET: a comprehensive platform integrating information on human disease-associated genes and variants. *Nucleic Acids Res.* **45**, D833–D839 (2017).
19. Szklarczyk, D. *et al.* STRING v10: protein-protein interaction networks, integrated over the tree of life. *Nucleic Acids Res.* **43**, D447–D452 (2015).
20. Shannon, P. *et al.* Cytoscape: a software environment for integrated models of biomolecular interaction networks. *Genome Res.* **13**, 2498–2504 (2003).
21. Mahalingam, D. *et al.* Targeting PIM kinase enhances the activity of sunitinib in renal cell carcinoma. *Br. J. Cancer* **105**, 1563–1573 (2011).
22. Lv, C., Bai, Z., Liu, Z., Luo, P. & Zhang, J. MicroRNA-495 suppresses human renal cell carcinoma malignancy by targeting SATB1. *Am. J. Transl. Res.* **7**, 1992–1999 (2015).
23. Pal, S.K. & Quinn, D.I. Differentiating mTOR inhibitors in renal cell carcinoma. *Cancer Treat. Rev.* **39**, 709–719 (2013).
24. Robb, V.A., Karbowniczek, M., Klein-Szanto, A.J. & Henske, E.P. Activation of the mTOR signaling pathway in renal clear cell carcinoma. *J. Urol.* **177**, 346–352 (2007).
25. Zhao, Q.D. *et al.* NADPH oxidase 4 induces cardiac fibrosis and hypertrophy through activating Akt/mTOR and NFkappaB signaling pathways. *Circulation* **131**, 643–655 (2015).
26. Wang, A.P. *et al.* miR-100 suppresses mTOR signaling in hypoxia-induced pulmonary hypertension in rats. *Eur. J. Pharmacol.* **765**, 565–573 (2015).
27. Torres, A. *et al.* Deregulation of miR-100, miR-99a and miR-199b in tissues and plasma coexists with increased expression of mTOR kinase in endometrioid endometrial carcinoma. *BMC Cancer* **12**, 369 (2012).
28. Corsini, L.R. *et al.* The role of microRNAs in cancer: diagnostic and prognostic biomarkers and targets of therapies. *Expert Opin. Ther. Targets* **16** (suppl. 2), S103–S109 (2012).
29. Zhou, H.C. *et al.* MicroRNAs miR-125b and miR-100 suppress metastasis of hepatocellular carcinoma by disrupting the formation of vessels that encapsulate tumour clusters. *J. Pathol.* **240**, 450–460 (2016).
30. Ivey, K.N. & Srivastava, D. microRNAs as developmental regulators. *Cold Spring Harb. Perspect. Biol.* **7**, a008144 (2015).
31. Jafari, N. *et al.* CRISPR-Cas9 mediated NOX4 knockout inhibits cell proliferation and invasion in HeLa cells. *PLoS One* **12**, e0170327 (2017).
32. Ishida, M. *et al.* MicroRNA-100 regulates a cluster of adipocytokine expression: a human biopsy study in subcutaneous and visceral adipose tissue. *Eur. Heart J.* **34** (suppl. 1), P3265 (2013).
33. Chen, D. *et al.* miR-100 induces epithelial-mesenchymal transition but suppresses tumorigenesis, migration and invasion. *PLoS Genet.* **10**, e1004177 (2014).
34. Liu, Y. *et al.* MiR-100 inhibits osteosarcoma cell proliferation, migration, and invasion and enhances chemosensitivity by targeting IGFIR. *Technol. Cancer Res. Treat.* **15**, NP40-NP48 (2016).
35. Jiang, Q. *et al.* MicroRNA-100 suppresses the migration and invasion of breast cancer cells by targeting FZD-8 and inhibiting Wnt/beta-catenin signaling pathway. *Tumour Biol.* **37**, 5001–5011 (2016).
36. Ge, Y.Y. *et al.* MicroRNA-100 promotes the autophagy of hepatocellular carcinoma cells by inhibiting the expression of mTOR and IGF-1R. *Oncotarget* **5**, 6218–6228 (2014).
37. Pankratz, F. *et al.* MicroRNA-100 suppresses chronic vascular inflammation by stimulation of endothelial autophagy. *Circ. Res.* **122**, 417–432 (2018).
38. Forte, M., Palmerio, S., Yee, D., Frati, G. & Sciarretta, S. Functional role of Nox4 in autophagy. *Adv. Exp. Med. Biol.* **982**, 307–326 (2017).
39. Steinhorn, B. *et al.* Insulin-dependent metabolic and inotropic responses in the heart are modulated by hydrogen peroxide from NADPH-oxidase isoforms NOX2 and NOX4. *Free Radic. Biol. Med.* **113**, 16–25 (2017).
40. Hanna, S.C., Heathcote, S.A. & Kim, W.Y. mTOR pathway in renal cell carcinoma. *Expert. Rev. Anticancer Ther.* **8**, 283–292 (2008).
41. Pal, K., Madamsetty, V.S., Dutta, S.K., Wang, E., Angom, R.S. & Mukhopadhyay, D. Synchronous inhibition of mTOR and VEGF/NRP1 axis impedes tumor growth and metastasis in renal cancer. *NPJ Precis. Oncol.* **3**, 31 (2019).
42. Nagaraja, A.K. *et al.* A link between mir-100 and FRAP1/mTOR in clear cell ovarian cancer. *Mol. Endocrinol.* **24**, 447–463 (2010).
43. Xu, C. *et al.* miRNA-100 inhibits human bladder urothelial carcinogenesis by directly targeting mTOR. *Mol. Cancer Ther.* **12**, 207–219 (2013).
44. Yu, Z., Li, N., Jiang, K., Zhang, N. & Yao, L.L. MiR-100 up-regulation enhanced cell autophagy and apoptosis induced by cisplatin in osteosarcoma by targeting mTOR. *Eur. Rev. Med. Pharmacol. Sci.* **22**, 5867–5873 (2018).